EXPERIMENTAL METHODS AND PROCESSING OF DATA

https://doi.org/10.46813/2023-145-033

DIGITAL STUDY OF THE $^{14}N(\gamma,2\alpha)^{6}Li$ REACTION

S.N. Afanasiev[1,], I.O. Afanasieva[2]*
[1]NSC "Kharkov Institute of Physics and Technology", Kharkiv, Ukraine;
[2]V.N. Karazin Kharkiv National University, Kharkiv, Ukraine
**E-mail: afanserg@kipt.kharkov.ua*

A digital measurement technique of points coordinates along the tracks was developed for the stereo frame photonuclear reaction data bank created in KIPT. The main procedure is the analysis of pixel intensity in the area of tracks. The $^{14}N(\gamma,2\alpha)^{6}Li$ reaction was chosen as a test reaction for measurement. A kinematic scheme for calculating the physical parameters of the reaction was created assuming a two-particle decay mode with the formation of an intermediate excited state. Experimental data and kinematic calculation were compared.

PACS: 25.20.-x

INTRODUCTION

Photoreactions on light nuclei are of particular interest to nuclear physics. They are driven by the well-known electromagnetic interaction and therefore their study provides important information about the fundamental properties of the nuclear forces. Photonuclear reactions are also important in nuclear fusion and astrophysical processes [1, 2]. It has been accepted [3, 4] that at quantum energies E_γ up to the meson threshold, nucleus absorption mainly occurs through two different reaction mechanisms: giant dipole resonance (at $E_\gamma < 40$ MeV) and quasi-deuteron photoabsorption (at $E_\gamma > 40$ MeV, where the photon wavelength is usually smaller than the nucleus size but close to the deuteron size). The (γ,N) and (γ,NN) reactions were qualitatively explained in the framework of various modifications of these interaction mechanisms. At the same time, in various nuclear reactions, not only protons and neutrons but also other particles such as deuterons, tritons, α-particles, and other light and heavy nuclei, different in composition and properties from the initial nucleus, are observed with significant probability. This led to the development of the model of the interaction of constituent nuclear particles (nucleon associations, cluster model) [5, 6]. The use of this theory made it possible to describe such effects that could not be explained by other methods. The simple cluster model assumes that the atomic nucleus consists of two structureless fragments whose properties coincide or are close to the properties of the corresponding nuclei in the free state. The two-cluster model assumes the presence of only two separate fragments – clusters, between which all nucleons of the nucleus are redistributed. The photon does not enter into strong nuclear interactions with the target nucleus, but only electromagnetic interactions with the cluster structure, the operators of which are exactly known. Therefore, it is possible to take into account only nuclear interactions of related clusters, which greatly simplifies the consideration in comparison with the three-body problem, when it is necessary to include the nuclear interaction of the incoming particle along with intercluster forces.

The ^{14}N nucleus is of interest as an intermediate between ^{12}C and ^{16}O nuclei, which in the cluster model are considered coupled systems of 3α- and 4α-particles. Previously, we have studied in detail the reactions of $^{12}C(\gamma,3\alpha)$ and $^{16}O(\gamma,4\alpha)$ [7]. In the present work, we present information on the $^{14}N(\gamma,2\alpha)^{6}Li$ reaction, which will provide new information on the evolution of the cluster structure, which becomes more complicated beyond α-clustering. The reaction $^{14}N(\gamma,2\alpha)^{6}Li$ has not been studied before, but nuclear reactions with such final particles in the literature are ($^{3}He + ^{11}B$ [8] and $d + ^{12}C$ [9]).

1. EXPERIMENTAL TECHNIQUE

The experiment was performed using a track 4π-detector (the diffusion chamber placed in a magnetic field with a strength of 1.5 T) [10]. The chamber was exposed to a beam of bremsstrahlung photons with a maximum energy of 150 MeV emitted from a linear electron accelerator (LUE-300). The soft component of the bremsstrahlung spectrum was removed by a beryllium filter 2.5 radiation-length units in thickness. The spectral distribution of photons was assumed to be of a Schiff form corrected for its nonuniform attenuation by the filter. To reduce the target density, the chamber was filled with a mixture of nitrogen (15%) and helium. This experimental method makes it possible to obtain, for slow final nuclei, track lengths acceptable for measurements and sufficiently high sharpness of their image at pressures close to atmospheric pressure. The target–detector combination made it possible to register the products of a low-energy reaction and analyze it practically from its threshold.

1.1. DIGITAL MEASUREMENT OF POINT COORDINATES ALONG TRACKS

In the experiment, during the sessions of irradiation of the camera, the working area of the camera was photographed by two 2-lens cameras. A large amount of information on multiparticle photoreactions was collected and an experimental complex with a digital data bank of stereo frames and a set of graphic programs that allow to restore events and perform physical analysis of the obtained data was created [11]. Photo frames have a structured name with the maximum necessary information about the experiment session.

In [11], a method of digital semi-automatic measurement of the coordinates of points along the

track was proposed. This allowed us to compare the digital method and the method using special devices. Also, the procedure of correct obtaining of physical information by digital measurement was created.

In this work, a fully automatic method of obtaining the kinematic parameters of particles is proposed, which reduces the contribution of the meter error and significantly speeds up the image processing.

For this purpose, a specialized graphical application was created using the Python programming language on the platform of the Tkinter graphics library with the use of additional modules – PIL, NumPy, SciPY, and Pandas. The PIL module allows you to access a two-dimensional array of numbers, which is a function of the image intensity distribution on the plane. The intensity range is from 0 (black) to 255 (white). The coordinate system starts in the upper left corner. The X coordinate increases from left to right, and the Y coordinate increases from top to bottom. Next, we will present algorithms for the mathematical processing of digital arrays (NumPy and SciPY) with further visualization of the results.

Fig. 1 shows two identical fragments of a photo frame with a three-beam event. The white segments emanating from the same vertex correspond to a three-beam event. It should be noted that there are significant background emissions (light objects in the frame) that can cause distortions during image analysis. They arise due to the complex gas structure of the diffusion chamber. However, such background emissions are not systematic and the total intensity along the tracks should be higher.

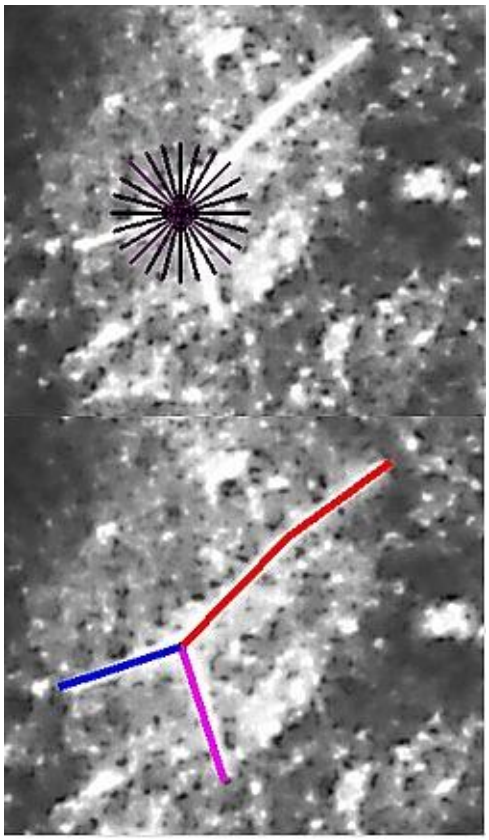

Fig. 1. Digital image processing

To implement an automatic technique for obtaining the kinematic parameters of reaction particles, we propose an algorithm that scans the intensity of pixels along a circular trajectory of a certain radius (Θ) and determines the average value at each scanning step $I_\Theta = (\sum_1^n I_i)/n$, where n is the number of pixels (radius length) and I_i is the intensity of the i-th pixel. In Fig. 1 above, for a visual example, dark segments of 50 pixels in length represent the procedure of scanning in a circle. The scan was performed along the clockwise trajectory with a step of 15 degrees. In the real study, the scanning step was 1°.

For the convenience of data analysis and searching for extremes, we introduced the relative intensity $I^{extr} = I_\Theta / I^{aver}$, where I^{aver} is the average intensity of the circle.

In Fig. 2, the histogram shows the dependence of Iextr on the scanning angle in the range from 0 to 360 degrees. There is an irregular structure with several maxima corresponding to the deviation from the background in the scanning area. To automatically determine the position of these maxima, we used the ***groupby()*** function from the Pandas module, which performs grouping by one or more parameters and determines the inflection points (extremes). The positions of the calculated extremes are shown as solid points. The three maxima in the positive region correspond to the three tracks in Fig. 1, and the position of the maximum gives the value of the departure angle of the corresponding track.

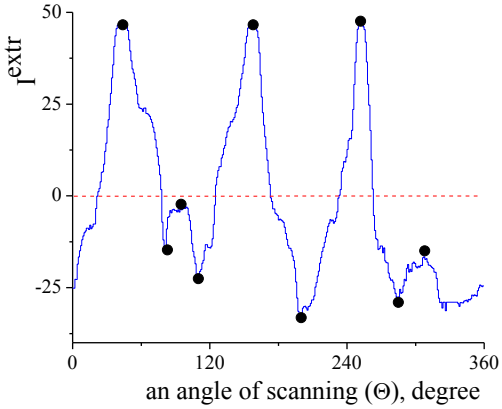

Fig. 2. Dependence of pixel intensity on scanning angle

Thus, knowing the top of the event, the angles of departure of the tracks, and the average intensity of the Icer in the selected direction, it is possible to calculate the coordinates of points along each track. For this purpose, the procedure of sequential advancement of the scanning segment along the corresponding track was performed. The pixels in the scanning segment were checked for intensity. A sharp change in intensity compared to I^{aver} made it possible to determine the boundary of the track. If all pixels corresponded to the track, the procedure was performed to move the start of the scan to the last point of the scanning segment, and then the procedure of scanning the intensity of pixels along a circular trajectory was performed again to determine the angle of departure of the track and further advancement along the track. This sequence of actions was performed in a loop until the track boundary was

determined. This algorithm allows us to take into account the curvature of the track and at each stage of moving along the track it is possible to refine the departure angle.

In Fig. 1 on the bottom image shows the result of the automatic digitization of all three event tracks. The points describe the trajectory of the tracks well. Subsequently, we performed the functions of fitting the points with a second-order linear curve and refining the coordinates of the middle of the track.

After reconstructing the geometry of the event, a numerical matrix of this event is created, in which for each track there are guide cosines l, m, n; the radius of curvature and track length.

1.2. $^{14}N(\gamma,2\alpha)^{6}LI$ REACTION EVENTS

For the measurement and processing of the $^{14}N(\gamma,2\alpha)^{6}Li$ reaction, we selected 3-ray stars close to compatibility, two of whose rays belong to two-charged particles and one to a three-charged particle. The ionization density, its change along the track at a known momentum, makes it possible to determine the charge of the particle. This identification was performed visually at the stage of selecting events for measurements. The particle tracks usually ended in the working area of the chamber, so the experimental data of their energy losses (energy-mileage ratio) were used to determine the kinetic energy of the particles [12]. The methodology for selecting events is traditional for this method of experiment and has been previously described [13, 14].

Events were identified after the measurement based on momentum balance. In the experiment, the axis OX was directed along the beam of γ-quanta. Boundary conditions were imposed on the quantities ΣP_x^i, ΣP_y^i, and ΣP_z^i, where $P_{x(y,z)}^i$ are the components of the three-dimensional momentum of the *i*-th final particle. The γ-quantum energy E_γ was determined as the sum of the kinetic energies of final particles and the reaction threshold. A distinctly pronounced peak in region 0 corresponded to events of the examined reaction. The energy and momentum conservation laws allowed the measurement results obtained for one of the tracks, which turned out to be the worst in comparison with the results obtained for all other tracks, to be made more exact. The measurement error of the momentum of charged particles depends on its size and track length and ranges from 3 to 10 %.

2. DATA PROCESSING

For the $^{14}N(\gamma,2\alpha)^{6}Li$ reaction events, the excitation energy of a pair of particles was determined as $E_x(\alpha\alpha) = M^{ef}(^{8}Be) - 2m_\alpha$, where $M^{ef}(^{8}Be)$ is the effective mass equal to the total energy of a pair of α-particles in their resting state, and m_α is the mass of the particle.

In Fig. 3, the histogram shows the distribution of $E_x(\alpha\alpha)$ with a step of 0.25 MeV. The distribution has a structure: a narrow near-threshold maximum and a concentration of events in the region of 3 MeV. The area of the first maximum is 15% of the total area.

There are three particles in the final state of the reaction, so three combinations of particle-pair systems are possible. This means that the structure observed in Fig. 3, is formed either by the decay of the intermediate excited state of the ^{8}Be nucleus or is simulated by one of the background pairs during the decay of the intermediate excited state of the ^{10}B nucleus.

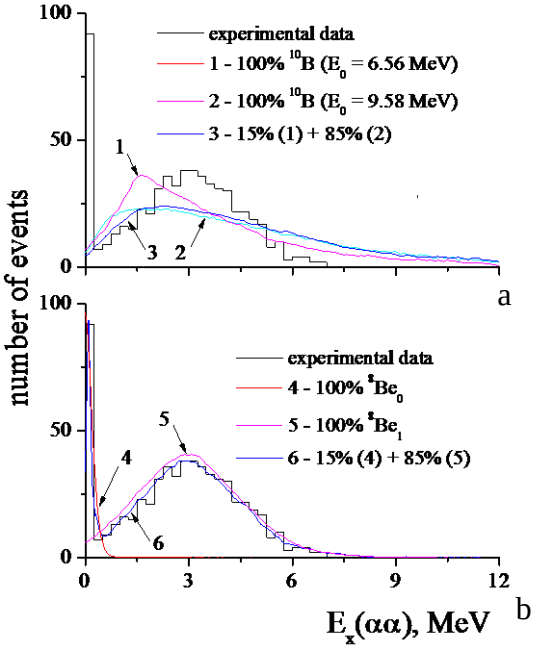

Fig. 3. Distribution of events by excitation energy of 2α-particles. The curves are explained in the text

At present, experimental studies of nuclear reactions on light nuclei are usually accompanied by a mathematical model of the process under study [15, 16].

2.1. KINEMATIC CALCULATION

To analyze the experimental data and compare it with the kinematic calculation, a graphical application in the Python programming language was created for this work. The matplotlib library is used for data visualization.

The kinematic model of the $^{14}N(\gamma,2\alpha)^{6}Li$ reaction was developed under the assumption of two-particle decay with the formation of an intermediate excited state. In the system of the center of mass (s.c.m.) of a two-particle reaction, the kinematics is determined by the fact that, regardless of the specific type of interaction, the reaction products scatter at an angle of 180^0 and have equal modulus momentum, and their energies in the same system depend only on the masses of the particles and the total energy of the system.

For the reaction of $^{14}N(\gamma,2\alpha)^{6}Li$, decay through two channels is possible

$$\gamma+^{14}N\rightarrow\alpha+^{10}B^*\rightarrow2\alpha^{6}Li, \quad (1)$$

$$\gamma+^{14}N\rightarrow^{8}Be^*+^{6}Li\rightarrow2\alpha^{6}Li. \quad (2)$$

The mathematical calculation is based on the literature data on the parameters of the levels of ^{10}B and ^{8}Be nuclei [17] and the corresponding assumptions about the angular distributions in the system of the reaction center of the particle that first left the ^{14}N nucleus and the particles in the intermediate state resting state. Each decay mode is reduced to three two-particle systems:

- ✓ $(\gamma+^{14}N)$ – initial,

- ✓ ($\alpha+^{10}B^*$) or ($^8Be^*+^6Li$) – intermediate,
- ✓ ($\alpha+^6Li$) or ($\alpha+\alpha$) – final.

To generate random values, a set of functions of the standard random library of the Python programming language was used. Several excited states of ^{10}B and ^8Be nuclei can contribute to the reaction. A scheme was created that allows you to select both the relative contribution for each channel (1) or (2) and the contribution of a separate level in each channel. To do this, we used the ***random.randint(0,100)*** function, which creates random, uncorrelated numbers evenly distributed in the range from 0 to 100. For the initial system, the numerical function of the distribution of the number of events on the energy of quanta $N(E_\gamma)$ was taken from a real experiment, and random values of E were generated by the ***random.choice()*** function. The excitation curves $f(E_x)$ of the ^{10}B and ^8Be states of the nuclei were taken as Gaussian functions with a maximum position E_0 and half-width at half-height (σ) from a compilation of spectroscopic data [17]. Random values were generated by the function ***random.gauss(E_0,σ)***.

In the non-relativistic approximation, in the system of the center of mass of the two-particle reaction $\gamma + {}^{14}N \rightarrow Z + Y^*$, the law of energy conservation is $E_\gamma = T_Z + T_Y + E_x(Y) + Q$, where T is the kinetic energy of particles Z and Y, $E_x(Y)$ is the excitation energy of the intermediate particle Y, and Q is the energy threshold of the $\gamma + {}^{14}N \rightarrow Z + Y$ reaction. Using the two-particle channel and the unambiguous connection between T_Z and T_Y, we obtain

$$T_Z = \frac{M_Y}{M_Z+M_Y}(E_\gamma - Q - E_x(Y)).$$

After the procedures for generating E_γ and $E_x(Y)$, T_Z and, accordingly, the particle momentum p_Z was determined.

The distributions over the polar angle Θ_Z for particle Z were taken in form $f(\Theta_Z) = c_1\cdot\sin^2\Theta_Z + c_2\cdot\sin^2\Theta_Z\cdot\cos\Theta_Z + c_3\cdot\sin^2\Theta_Z\cdot\cos^2\Theta_Z + c_4$, where $c_{1\text{-}4}$ are coefficients containing information about the reaction mechanism and wave functions of the nuclei. Parameters $c_{1\text{-}4}$ were determined from the quantum values of the intermediate excited nucleus [18]. The distribution in the azimuthal angle Θ_Z is isotropic and was generated by multiplying the random number ***random.randint(0,1)*** by 2π.

The polar (Θ_Z) and azimuthal (φ_Z) angles were generated and the longitudinal and transverse projections of the momentum of particle Z were determined. The values of the projections and the total momentum of nucleus Y were calculated from the two-particle process.

A similar procedure was carried out for the final system, provided that the energy of the system is the excitation energy of the particle Y. The kinematic parameters of the particles were transferred from the s.c.m. reaction to the laboratory reference frame. The laws of conservation of energy and momentum for the kinematic parameters of the particles were checked. An event was considered formed if it satisfied the conservation laws.

2.2. DISCUSSION OF THE RESULTS

For example, let us compare the kinematic calculation with the experiment (see Fig. 3).

Using the kinematic model, we constructed several distributions of events according to $E_x(\alpha\alpha)$ under the assumption of each decay channel – (1) or (2).

In Fig. 3,a, three curves are presented in the framework of decay through a channel (1): curve 1 – with 100 % production of the narrow ^{10}B nucleus level (E_0 = 6.56 MeV, σ = 0.025 MeV); curve 2 – with 100% formation of the broad ^{10}B nucleus level (E_0 = 9.58 MeV, σ = 0.257 MeV); curve 3 – with 15% of the narrow ^{10}B nucleus level and 85% of the broad ^{10}B nucleus level formation.

The dependence of 15 and 85% is taken from the ratio of the areas of the maxima in the experiment. The calculated curves were normalized to the experimental distribution by area. The curves do not fully describe the near-threshold maximum. In addition, they give only one maximum, which has almost the same position (at 1.5 MeV) with different widths. It was checked that any combinations of the relative contributions of curves 1 and 2 also do not describe the experimental distribution.

Two levels of ^8Be nucleus were chosen for a channel (2): the ground state (GS) with E_0 = 0.092 MeV, σ = 0.025 MeV, and 1^e excited state with E_0 = 3.04 MeV, σ = 0.75 MeV. Fig. 3,b shows three curves corresponding to the following ratios: curve 4 – with 100% OS; curve 5 – with 100% of the 1^{st} level of the ^8Be nucleus; curve 6 – with 15% GS and 85% of the 1^{st} level of the ^8Be nucleus.

Curves 4 and 5 are consistent with the experiment when describing the first and second maxima, respectively. And curve 6 satisfactorily describes the entire experimental distribution.

Thus, it can be concluded that in the $^{14}N(\gamma,2\alpha)^6Li$ reaction, decay occurs mainly through the formation of an intermediate excited ^8Be nucleus. In the future, it is planned to separate the events corresponding to the formation of the GS and the 1^{st} excited state of the ^8Be nucleus and to analyze the experimental data for each partial channel.

3. CONCLUSIONS

A systematic study of the $^{14}N(\gamma,2\alpha)^6Li$ reaction was performed. To obtain the physical parameters of events, a graphical application with the ability to automatically measure the coordinates of points along tracks on digital photographs was created in the Python programming language. The main procedure is to analyze the intensity of pixels in the area of tracks along a circular trajectory of a certain radius.

The excitation energy of the 2α-particle system is determined and a structure with two maxima is detected. The structure is formed either as a result of the decay of the intermediate excited state of the ^8Be nucleus or is simulated by one of the background pairs during the decay of the intermediate excited state of the ^{10}B nucleus.

A kinematic scheme for calculating the physical parameters of the reaction has been developed in the assumption of a two-particle decay mode with the formation of an intermediate excited state. A comparison of experimental data and kinematic calculation was performed and it was determined that the decay process with the formation of an intermediate excited ^{8}Be nucleus in the ground and 1st excited states is carried out with high reliability.

REFERENCES

1. A. Coc, C. Angulo, E. Vangioni-Flam, et al. Big Bang nucleosynthesis, microwave anisotropy, and the light element abundances // *Nucl. Phys. A.* 2005, v. 752, p. 522-531, https://doi.org/10.1016/-j.nuclphysa.2005.02.057.
2. F.K. Thielemann, F. Brachwitz, C. Freiburghaus, et al. Element synthesis in stars // *Prog. Part. Nucl. Phys.* 2001, v. 46, p. 5-22, https://doi.org/10.1016/-S0146-6410(01)00103-X
3. E.G. Fuller. Photonuclear reaction cross sections for ^{12}C, ^{14}N and ^{16}O // *Physics Reports*. 1985, v. 127, p. 185-231, https://doi.org/10.1016/0370-1573(85)90145-0
4. D.J.S. Findlay. Applications of photonuclear reactions // *Nucl. Instr. and Meth. in Phys. Res. Section B: Beam Interactions with Materials and Atoms*. 1990, v. 50, p. 314-320, https://doi.org/-10.1016/0168-583X(90)90374-4
5. O.F. Nemets, V.G. Neudachin, A.T. Rudchik, et al. *Nuklonnyye assotsiatsii v legkikh yadrakh i yadernyye reaktsii mnogonuklonnykh peredach*. Kiev: "Naukova Dumka", 1988, 488 p. (in Russian).
6. M. Freer, H. Horiuchi, Y. Kanada-En'yo, et al. Microscopic clustering in light nuclei // *Rev. Mod. Phys.* 2018, v. 90, p. 035004, https://doi.org/-10.1103/RevModPhys.90.035004
7. S.N. Afanasyev. Energy correlations of α-particles in the ^{8}Be-nucleus ground state formation channel of the ^{12}C(γ,3α) and ^{16}O(γ,4α) reactions // *Ukr. J. Phys.* 2019, v. 64, No. 9, p. 787-792, https://doi.org/10.15407/ujpe64.9.787
8. F.C. Young, P.D. Forsyth, J.B. Marion. The ^{11}B(^{3}He,^{6}Li)^{8}Be reaction // *Nucl. Phys. A.* 1967, v. 91, p. 209-221, https://doi.org/10.1016/0375-9474(67)90462-9
9. L. Jarczyk, B. Kamys, Z. Rudy, et al. Highly excited ^{8}Be core in the configuration of the ^{12}C and ^{11}B ground states // *Nucl. Phys. A.* 1986, v. 459, p. 52-60, https://doi.org/10.1016/0375-9474(86)-90055-2
10. Yu.M. Arkatov, P.I. Vatset, V.I. Voloshchuk, et al. Setup for the study of photonuclear reactions // *Prib. Tekh. Eksp.* 1969, v. 3, p. 205 (in Russian).
11. S.N. Afanasiev, I.A. Afanasieva. Digital processing of photos from 4π track detector // *Problems of Atomic Science and Technology. Series "Nuclear Physics Investigations"*. 2022, No. 5(141), p. 87-91, https://doi.org/10.46813/2022-141-087
12. O.F. Nemets, Yu.V. Gofman. *Handbook of Nuclear Physics* Kiev: "Naukova Dumka", 1975, 416 p.
13. V.V. Kirichenko, A.F. Khodyachikh, P.I. Vatset, et al. Investigation of the reactions of ^{12}C(γ,pα)^{7}Li and ^{12}C(γ,nα)^{7}Be at $E_{\gamma}^{max} \leq 120$ MeV // *Yad. Fiz.* 1979, v. 29, p. 572-581.
14. S.N. Afanasyev, A.F. Khodyachikh. On the formation mechanism of excited states of the ^{8}Be nucleus in the ^{12}C(γ,3α) reaction // *Yad. Fiz.* 2008, v. 71, p. 1859-1869, https://doi.org/10.1134/-S106377880811001X
15. D. Dell'Aquila, I. Lombardo, G. Verde, et al. Phys. High-Precision Probe of the Fully Sequential Decay Width of the Hoyle State in ^{12}C // *Phys. Rev. Lett.* 2017, v. 119, p. 132501, https://doi.org/10.1103/-PhysRevLett.119.132501
16. S.N. Afanasyev. Modeling of the kinematics of multiparticle photoreaction in the framework of a sequential two-particle process // *Proceedings of the 5rd International Conference "Computer modeling of high-technology (CMHT-2018)"*. 2018, p. 37-40.
17. D.R. Tilley, J.H. Kelley, J.L. Godwin, et al. Energy levels of light nuclei A = 8, 9, 10 // *Nucl. Phys. A*. 2004, v. 745, p. 155-362, https://doi.org/10.1016/-j.nuclphysa.2004.09.059
18. A.M. Baldin, V.I. Gol'danskii, V.M. Maksimenko, I.L. Rosenthal. *Kinematics of Nuclear Reactions*. M.: "Atomizdat", 1968, 456 p.

Article received 07.03.2023

ЦИФРОВЕ ДОСЛІДЖЕННЯ РЕАКЦІЇ ^{14}N(γ,2α)^{6}Li

С.М. Афанасьєв, І.О. Афанасьєва

Для створеного в ННЦ ХФТІ банку даних стереокадрів фотоядерних реакцій розроблено методику цифрового вимірювання координат точок уздовж треків. Основною процедурою є аналіз інтенсивності пікселів у області треків. Як тестову для вимірювання обрано реакцію ^{14}N(γ,2α)^{6}Li. Створено кінематичну схему розрахунку фізичних параметрів реакції в припущенні двочастинкової моди розпаду з утворенням проміжного збудженого стану. Виконано порівняння експериментальних даних і кінематичного розрахунку.